The Plant Cell, Vol. 15, 1333–1346, June 2003, www.plantcell.org © 2003 American Society of Plant Biologists

PAA1, a P-Type ATPase of Arabidopsis, Functions in Copper Transport in Chloroplasts

Toshiharu Shikanai,[a,1] Patricia Müller-Moulé,[b] Yuri Munekage,[a] Krishna K. Niyogi,[b] and Marinus Pilon[c]

[a] Graduate School of Biological Sciences, Nara Institute of Science and Technology, Ikoma, Nara 630-0101, Japan
[b] Department of Plant and Microbial Biology, University of California, Berkeley, California 94720-3102
[c] Biology Department, Colorado State University, Fort Collins, Colorado 80523

Copper (Cu) is an essential trace element with important roles as a cofactor in many plant functions, including photosynthesis. However, free Cu ions can cause toxicity, necessitating precise Cu delivery systems. Relatively little is known about Cu transport in plant cells, and no components of the Cu transport machinery in chloroplasts have been identified previously. Cu transport into chloroplasts provides the cofactor for the stromal enzyme copper/zinc superoxide dismutase (Cu/ZnSOD) and for the thylakoid lumen protein plastocyanin, which functions in photosynthetic electron transport from the cytochrome b_6f complex to photosystem I. Here, we characterized six Arabidopsis mutants that are defective in the *PAA1* gene, which encodes a member of the metal-transporting P-type ATPase family with a functional N-terminal chloroplast transit peptide. *paa1* mutants exhibited a high-chlorophyll-fluorescence phenotype as a result of an impairment of photosynthetic electron transport that could be ascribed to decreased levels of holoplastocyanin. The *paa1-1* mutant had a lower chloroplast Cu content, despite having wild-type levels in leaves. The electron transport defect of *paa1* mutants was evident on medium containing <1 μM Cu, but it was suppressed by the addition of 10 μM Cu. Chloroplastic Cu/ZnSOD activity also was reduced in *paa1* mutants, suggesting that PAA1 mediates Cu transfer across the plastid envelope. Thus, PAA1 is a critical component of a Cu transport system in chloroplasts responsible for cofactor delivery to plastocyanin and Cu/ZnSOD.

INTRODUCTION

Copper (Cu) is a redox-active transition metal that plays critical roles in diverse reduction and oxidation reactions, including photosynthetic electron transport (Raven et al., 1999), respiration, oxidative stress responses, and hormone signaling. Despite its physiological importance to plants (for a review of the effects of Cu nutrition on plants, see Marschner, 1995), Cu shows visible toxicity to Arabidopsis plants grown on agar medium at concentrations as low as 20 μM (Murphy and Taiz, 1995). To avoid metal ion–induced damage, all living organisms have evolved mechanisms to avoid the accumulation of free metal ions in cells while still delivering sufficient cofactors to target proteins (Nelson, 1999). For example, in yeast, the concentration of free Cu is $<10^{-18}$ M, representing less than one atom per cell (Rae et al., 1999), whereas the total Cu concentration in yeast is ~70 μM. This situation probably reflects the very high chelating capacity for Cu within cells and underscores the existence of binding proteins and membrane transporters with high affinity and specificity.

In plants, relatively little is known about Cu transport into and within cells, although several families of heavy metal transporters have been identified (for reviews, see Fox and Guerinot, 1998; Himelblau and Amasino, 2000; Williams et al., 2000). The Arabidopsis *COPT1* gene and its homologs encode Cu transporters that allow the entrance of Cu into cells (Kampfenkel et al., 1995; Sancenon et al., 2003). Components of intracellular Cu transport and trafficking identified in Arabidopsis include metallothioneins (Zhou and Goldsbrough, 1994), a possible Cu chaperone, *CCH* (Himelblau et al., 1998), that is homologous with yeast *ATX1* (Lin et al., 1997; Pufahl et al., 1997), and *RAN1* (Hirayama et al., 1999), a homolog of the yeast and human genes that encode Cu-transporting P-type ATPases that function in the endomembrane system. Ethylene receptors are equipped with Cu in a late secretory system compartment, and the Arabidopsis mutant *ran1* was identified based on its aberrant response to an ethylene antagonist, allowing the positional cloning of the gene (Hirayama et al., 1999). Three putative Cu-transporting P-type ATPases other than RAN1 have been identified in the Arabidopsis genome (Axelsen and Palmgren, 2001), but their functions have not yet been elucidated.

In cyanobacteria, which are thought to be related to the evolutionary ancestor of the chloroplast, two Cu-transporting P-type ATPases have been found. PacS (Kanamaru et al., 1994) and CtaA (Phung et al., 1994) supply Cu for photosynthesis and are required for holoplastocyanin formation (Tottey et al., 2001). PacS is located in thylakoid membranes (Kanamaru et al., 1994), whereas CtaA is believed to be located in the cyanobacterial cytoplasmic membrane (Tottey et al., 2001). A Cu chaperone, Atx1, has been discovered that may acquire Cu from either CtaA or other sources in the cyanobacterial cytosol and donate Cu to PacS (Tottey et al., 2002). In Arabidopsis, PAA1, a member of the metal-transporting P-type ATPase family, was identified originally by its sequence similarity to cyanobacterial

[1] To whom correspondence should be addressed. E-mail shikanai@bs.aist-nara.ac.jp; fax 81-743-72-5489.
Article, publication date, and citation information can be found at www.plantcell.org/cgi/doi/10.1105/tpc.011817.

PacS (Tabata et al., 1997). In view of the similarity between plastids and cyanobacteria, P-type ATPases such as PAA1, which are more similar to cyanobacterial transporters than to RAN1, may be responsible for Cu delivery to chloroplasts.

Understanding how Cu is delivered to chloroplast proteins such as plastocyanin and copper/zinc superoxide dismutase (Cu/ZnSOD) is of particular interest because of the important role of these proteins in photosynthesis and the significance of photosynthesis to plant productivity. Plastocyanin is an abundant Cu protein in the thylakoid lumen of higher plants that functions in electron transport between the cytochrome b_6f complex and photosystem I (PSI). It is synthesized in the cytosol as a precursor with organelle-targeting information (Smeekens et al., 1985). Because the chloroplast protein import machinery has a strong unfolding capacity (Guera et al., 1993; America et al., 1994), proteins such as plastocyanin are thought to acquire their cofactors after import into the organelle (for review, see Merchant and Dreyfuss, 1998). De novo cofactor insertion into plastocyanin was observed after in vitro translocation into the lumen (Li et al., 1990). The plastocyanin polypeptide is unstable in *Chlamydomonas reinhardtii* grown in Cu-deficient medium (Merchant and Bogorad, 1986; Li and Merchant, 1995), and under these conditions, a cytochrome c_6 is induced that functionally replaces plastocyanin. A mutant strain of Chlamydomonas has been described that accumulates apoplastocyanin (without the Cu cofactor) when grown in Cu-supplemented medium, but the gene has not been identified (Li et al., 1996). Arabidopsis expresses two plastocyanin genes that encode proteins that are closely related in sequence (Vorst et al., 1988; Schubert et al., 2002). In contrast to past dogma, plastocyanin is not absolutely essential for photosynthesis and viability in Arabidopsis, because a constitutively expressed cytochrome c_6 can partially replace plastocyanin function (Gupta et al., 2002). However, elimination of both plastocyanins and cytochrome c_6 is lethal (Gupta et al., 2002).

Cu also is a cofactor of isoforms of Cu/ZnSOD, enzymes that serve to reduce oxidative stress (for reviews, see Bowler et al., 1992, 1994). In Arabidopsis, three isozymes of Cu/ZnSOD are found (Kliebenstein et al., 1998). The two main isoforms are present in the cytosol (CSD1) and the chloroplast stroma (CSD2). Like plastocyanin, stromal Cu/ZnSOD is encoded by a nuclear gene, and the polypeptide is translocated across the envelope, probably before the insertion of the cofactor. A third isozyme (CSD3) is thought to be present in peroxisomes. Polyphenol oxidase is a Cu protein that is detected in the thylakoid lumen of some plants, such as spinach (Kieselbach et al., 1998), but it is not found in the thylakoid lumen of Arabidopsis (Schubert et al., 2002). Other important Cu proteins of known function include cytochrome *c* oxidase in mitochondria (Ferguson-Miller and Babcock, 1996) and the ethylene receptors (Rodriguez et al., 1999).

In this study, we characterized six mutant alleles of the Arabidopsis *PAA1* gene that have a high-fluorescence phenotype caused by a defect in photosynthetic electron transport. The mutant plants had normal levels of Cu in their shoots but were impaired in Cu delivery to chloroplasts, affecting both stromal Cu/ZnSOD activity and plastocyanin. We show that PAA1 contains a functional chloroplast-targeting sequence and that it is a critical component of a Cu transport system responsible for cofactor delivery to chloroplast Cu proteins.

RESULTS

Isolation of Arabidopsis *paa1* Mutants Exhibiting High Chlorophyll Fluorescence

Using a fluorescence imaging system (Niyogi et al., 1998; Shikanai et al., 1999), six Arabidopsis mutants displaying a similar high-chlorophyll-fluorescence phenotype were isolated (Figure 1). Genetic crosses revealed that the phenotype of each of the mutants, two in the Landsberg *erecta* (L*er*) background and four in the Columbia (Col) background, was attributable to a recessive mutation in a nuclear gene. By crossing the mutants to each other, the six mutants were placed into a single complementation group. These mutant alleles were named after the gene later found to be responsible for the phenotype, *PAA1*, for P-type ATPase in Arabidopsis (see below; Tabata et al., 1997). *paa1-1*, *paa1-2*, and *paa1-4*, which were first described as recessive mutants with reduced electron transport activity, were referred to originally as LE17-8, LE17-11, and CE10-10-2, respectively (Shikanai et al., 1999). All six *paa1* alleles exhibited a reduced growth rate, even at low light intensity (40 μmol·m^{-2}·s^{-1}) (Figure 1). The reduction in the growth rate was pronounced on MS medium (Murashige and Skoog, 1962) (Table 1).

The *paa1* Mutants Are Defective in Photosynthetic Electron Transport

The high-chlorophyll-fluorescence phenotype of the *paa1* mutants suggested a defect in photosynthetic electron transport; therefore, we determined the light-intensity dependence of two chlorophyll fluorescence parameters, the electron transport rate (ETR) and nonphotochemical quenching (NPQ). ETR esti-

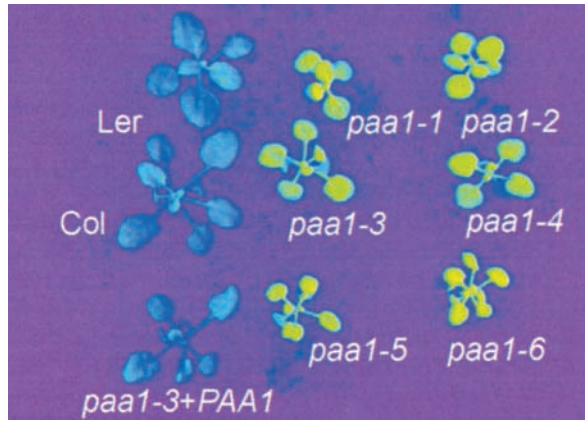

Figure 1. Chlorophyll Fluorescence Imaging.

Wild-type and *paa1* seedlings were grown in soil for 4 weeks. A chlorophyll fluorescence image was captured after 1 min of illumination with actinic light (300 μmol·m^{-2}·s^{-1}). False coloring represents the fluorescence level in the following order: yellow > green > light blue > dark blue. Col, Columbia *gl1* wild type; L*er*, Landsberg *erecta* wild type; *paa1-3* + *PAA1*, *paa1-3* transformed with the genomic *PAA1* sequence.

Table 1. Fresh Weights of 3-Week-Old Seedlings

Genotype	Fresh Weight (mg)
L*er*	27.3 ± 5.6
Col	25.2 ± 6.2
paa1-1 (L*er*)	4.4 ± 1.8
paa1-3 (Col)	4.1 ± 1.7
paa1-3 + *PAA1*	30.0 ± 11.0

Values shown are averages from 10 to 11 measurements.

mates the rate of PSII electron transport, whereas NPQ is a measure of photoprotective feedback deexcitation of excess light energy. Figure 2 shows that the maximum ETR in *paa1* was ~30% of that of the wild type. In *paa1*, ETR was affected even at a low light intensity (50 μmol·m^{-2}·s^{-1}), which explains the reduced growth rate. The ETR was saturated at a relatively low light intensity (100 to 200 μmol·m^{-2}·s^{-1}) in *paa1*, whereas saturation occurred at ~700 μmol·m^{-2}·s^{-1} in the wild type (Figure 2, top graphs). NPQ induction also was affected severely in *paa1* (Figure 2, bottom graphs). Because the major component of NPQ depends on the accumulation of a high transthylakoid ΔpH (for review, see Müller et al., 2001), this result suggests that the ΔpH formed by electron transport in *paa1* during steady state photosynthesis is not sufficient to induce NPQ even at high light intensities. A reduced accumulation of the proton gradient was supported by the observation that ΔpH-dependent zeaxanthin accumulation at saturating light intensity was reduced in *paa1* relative to the wild type (data not shown). Thus, the high-chlorophyll-fluorescence phenotype in *paa1* was attributable to decreases in both photochemical and nonphotochemical quenching of chlorophyll fluorescence.

To characterize the *paa1* mutants with respect to defects in the electron transport pathway, the redox levels of both photosystems were determined during steady state photosynthesis (Figure 3). The 1 − qP parameter is an indication of the oxidation state of the quinone acceptor of PSII (Schreiber et al., 1986). In the wild type, the quinone acceptor of PSII (Q_A) exists mostly in the oxidized state under low light and becomes more reduced when the light intensity is increased. In *paa1*, Q_A was more reduced than in the wild type at any light intensity, consistent with a defect in the electron transport chain after PSII (Figure 3, top graphs). The 1 − (ΔA/ΔAmax) parameter is indicative of the oxidation state of the special pair of reaction center chlorophylls in PSI (P700). In wild-type plants, these chlorophylls become more oxidized with increases in light intensity. This effect is ascribed to the downregulation of PSII photochemistry by NPQ and the restriction of electron transport at

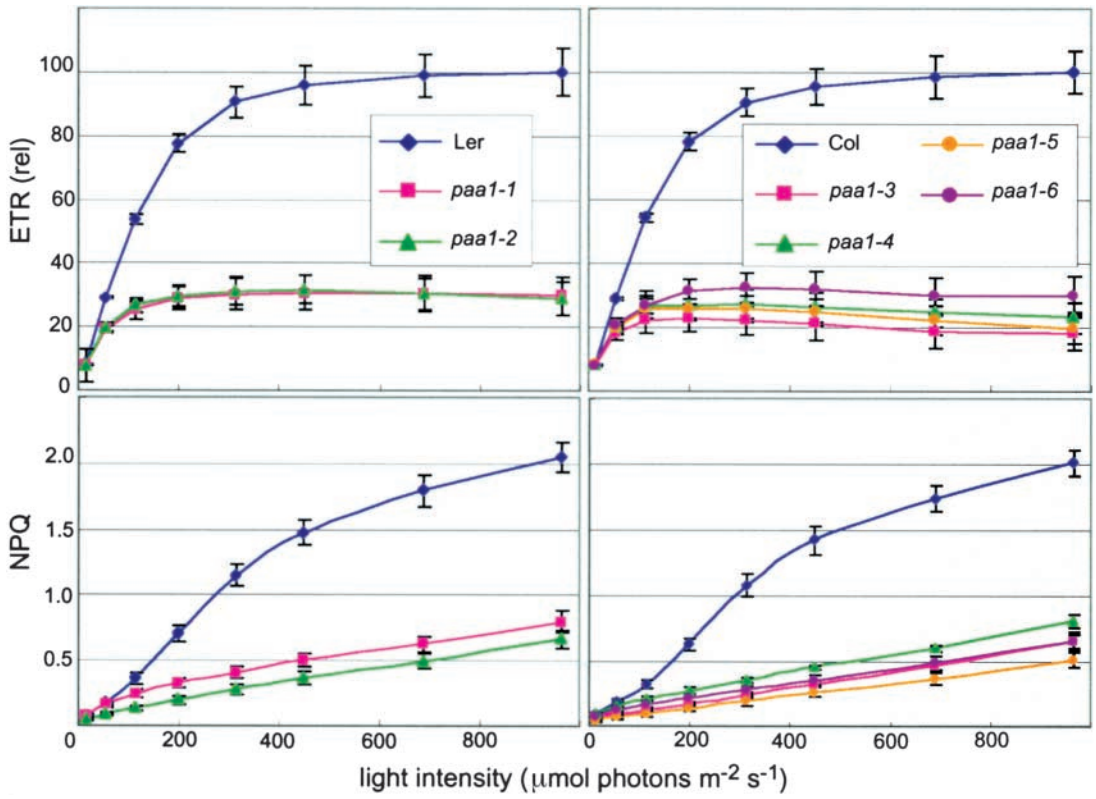

Figure 2. Light-Intensity Dependence of Steady State Chlorophyll Fluorescence Parameters.

ETR is depicted relative (rel) to a value of 100 for the maximum ETR in the wild type (top graphs). The bottom graphs show the light-intensity dependence of NPQ. Data for mutants in the L*er* background are shown at right, and data for mutants in the Col background are shown at left. Each point represents the mean ± SD (n = 5).

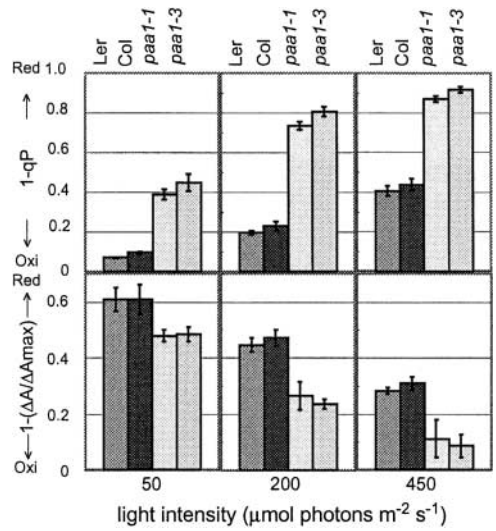

Figure 3. Steady State Redox Levels of the Two Photosystems.

Redox states of the primary quinone-type electron acceptor, Q_A, of PSII were determined by a chlorophyll fluorescence parameter, 1 − qP. Redox states of reaction center chlorophylls of PSI (P700) were determined by absorbance changes at 820 nm [1 − (ΔA/ΔAmax)]. For both parameters, values of 1 and 0 correspond to full reduction (Red) and full oxidation (Oxi), respectively. Each bar represents the mean ± SD (n = 5).

the cytochrome b_6f complex. Despite the NPQ defect in the mutants (Figure 2), P700 was more oxidized in *paa1* than in the wild type, indicating that electron transport is restricted more severely before P700 in *paa1* (Figure 3, bottom graphs). These results suggest that electron transport in *paa1* is limited between Q_A in PSII and P700 in PSI, possibly at plastoquinone, the cytochrome b_6f complex, or plastocyanin.

The *paa1* Mutations Map to a Gene That Encodes a Metal-Transporting P-Type ATPase

The gene affected in the *paa1* mutants was identified by map-based cloning. The *paa1-1* mutant (L*er* background) was crossed to a polymorphic wild-type strain (Col), and the mutation was mapped between molecular markers g8300 and nga1139 on chromosome 4 (Figure 4). Fine mapping using 141 F2 plants identified a 280-kb region covered by four BAC clones (F26P21, F4I10, F17M5, and T16L1). The genomic sequences of candidate genes that encode predicted chloroplast-targeted proteins were determined, and sequence alterations were found in a single gene, At4g33525, in all *paa1* alleles (Figures 4 and 5). At4g33525 encodes a possible metal-transporting P-type ATPase (Solioz and Vulpe, 1996), which was identified originally as a homolog of cyanobacterial PacS (Kanamaru et al., 1994; Tabata et al., 1997). To verify that the *paa1* phenotype is the result of mutations in At4g33525, a wild-type genomic clone of At4g33525 was introduced into *paa1-3*. This gene fully complemented both the chlorophyll-fluorescence and growth-rate phenotypes when transformed into *paa1-3* (Figure 1, Table 1, *paa1-3* + *PAA1*), confirming that the defects observed in our mutants were caused by lesions in *PAA1*.

PAA1 is a member of the metal-transporting P-type ATPase family, which is characterized by the presence of a short GMxCxxC consensus metal binding motif in the N-terminal region, and it is most similar to known Cu-transporting P-type ATPases (Tabata et al., 1997; Axelsen and Palmgren, 2001). In Arabidopsis, four possible Cu-transporting P-type ATPases are encoded, and Figure 5 shows an alignment of these four predicted protein sequences along with the sequences of two Cu-transporting P-type ATPases from the cyanobacterium *Synechocystis* sp strain PCC6803, PacS and CtaA (Tottey et al., 2001). RAN1 is the best characterized P-type ATPase in Arabidopsis, functioning in Cu delivery to the ETR1 ethylene receptor in a late secretory compartment (Hirayama et al., 1999; Woeste and Kieber, 2000). HMA5 (At1g63440), which has a possible mitochondrial presequence, is most similar to RAN1 (48% sequence identity). RAN1 and HMA5 have two metal binding domains in the N-terminal regions of the proteins, whereas PAA1 and PAA2 (At5g21930) each has only one, similar to CtaA and PacS. PAA2 shows high similarity to PAA1 (43% identity), and both proteins have possible chloroplast transit sequences. PAA1 is slightly more similar to CtaA (42% identity) than to PacS (38% identity).

In addition to their N-terminal metal binding domains, P-type ATPases contain several other conserved domains. These domains are a phosphatase domain, an ion transduction domain, a phosphorylation domain, and an ATP binding domain (Solioz and Vulpe, 1996; Axelsen and Palmgren, 2001). A nonsense mutation was found in *paa1-1* in the eighth exon, which should lead to the truncation of the C-terminal region containing the ion transduction, phosphorylation, and ATP binding domains. This result suggests that *paa1-1* might be a null allele that lacks PAA1 activity. *paa1-4* had a nonsense mutation in the 15th exon, which could lead to the lack of the final two predicted transmembrane regions. *paa1-3* had an in-frame deletion of

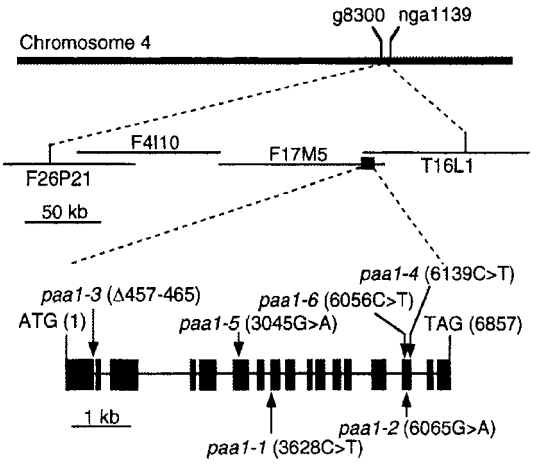

Figure 4. Positional Cloning of *paa1*.

paa1 was mapped to the 280-kb region spanning four BAC clones on chromosome 4. The small box on F17M5 represents the position of *PAA1*. Exons (boxes) and introns (lines) were predicted from the cDNA sequence (Tabata et al., 1997). Arrows indicate positions of the *paa1* mutations.

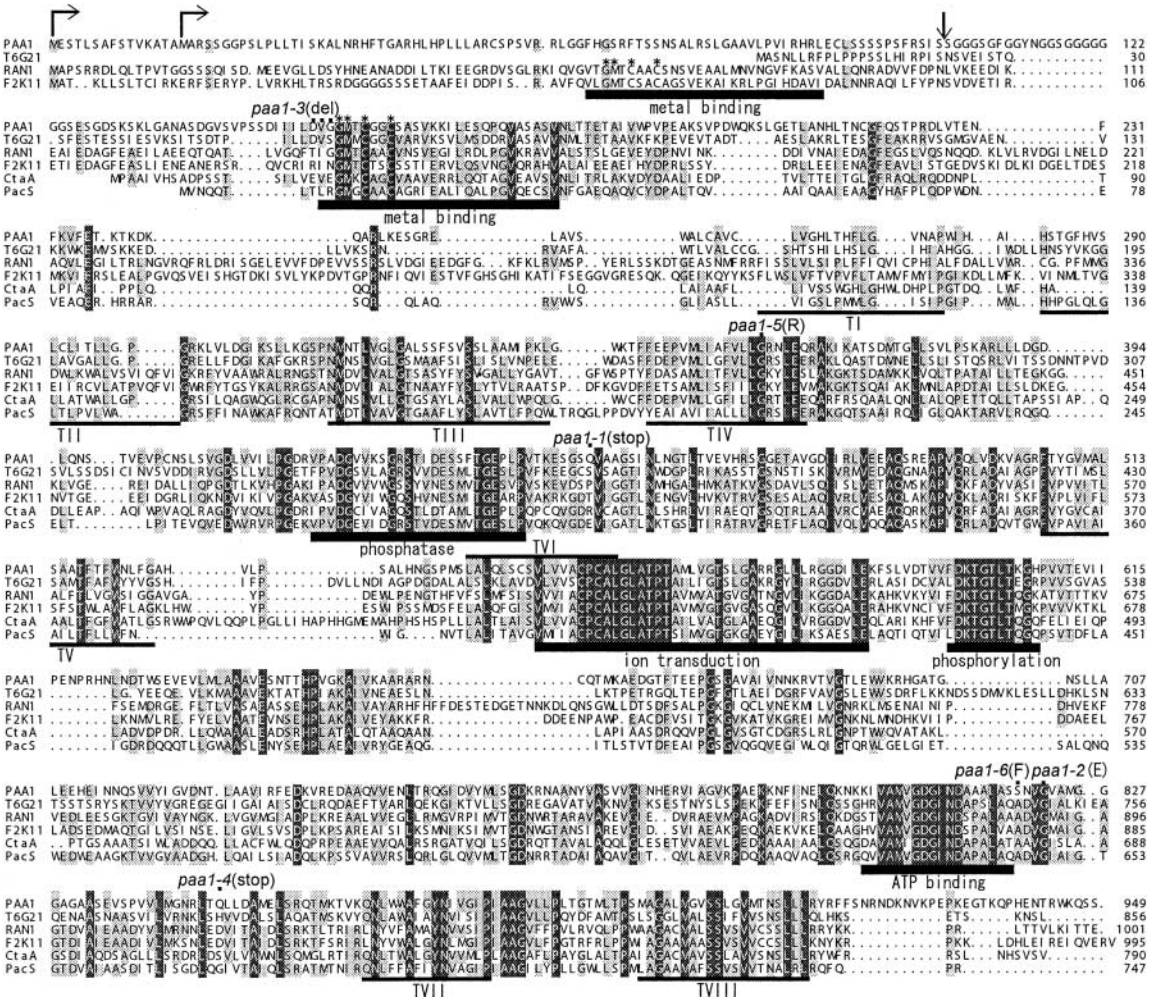

Figure 5. Alignment of Cu-Transporting P-Type ATPase Sequences.

Alignment of PAA1 with three other Cu-transporting P-type ATPases from Arabidopsis, RAN1, PAA2 (At5g21930/T6G21), and HMA5 (At1g63440/F2K11), and two from *Synechocystis* sp strain PCC6803, CtaA and PacS. Cu-transporting activity has not been assessed in PAA2 or HMA5. Thick bars indicate predicted functional domains. Eight possible transmembrane domains are shown by thin bars (TI to TVIII). Dots on the sequence indicate the positions of *paa1* mutations. The conserved GMxCxxC motifs are indicated by asterisks. Two possible in-frame initiation codons are indicated by horizontal arrows. A predicted processing site (TargetP) of the transit peptide is indicated by a vertical arrow.

three amino acids in the metal binding domain, adjacent to the conserved GMxCxxC motif. By contrast, *paa1-2* and *paa1-6* had alterations in amino acids that were adjacent to the ATP binding domain. *paa1-5* had an alteration in the well-conserved Gly residue located in the fourth transmembrane region. All of these mutations must have critical effects on PAA1 function, because the phenotype is very similar among all six alleles, including the likely null allele, *paa1-1*.

PAA1 Contains a Functional Cleavable Chloroplast Transit Sequence

The photosynthetic electron transport defect of *paa1* mutants suggested that PAA1 is likely to function in Cu transport in chloroplasts; therefore, we determined whether *PAA1* encodes a precursor with an N-terminal cleavable chloroplast transit sequence. The 5′ region of *PAA1* contains two possible in-frame initiation codons (encoding Mets corresponding to residues 1 and 16 in Figure 5), either of which could function as a translational start site. To test the functionality of the possible chloroplast transit sequences beginning at either start site, we constructed two fusions of the N terminus of PAA1 with a passenger protein. As a passenger, we chose the mature sequence of plastocyanin from *Silene pratensis*, which lacks its own targeting information (Smeekens et al., 1986). In one fusion construct, the coding sequence for 109 amino acids of PAA1 starting from the first initiation codon was present (Figure 6, Paa1Ltp-PC). In the second fusion, only the coding sequence for the 94 amino acids of PAA1 starting from the second initiation codon was present (Figure 6, Paa1Stp-PC). Fusion pro-

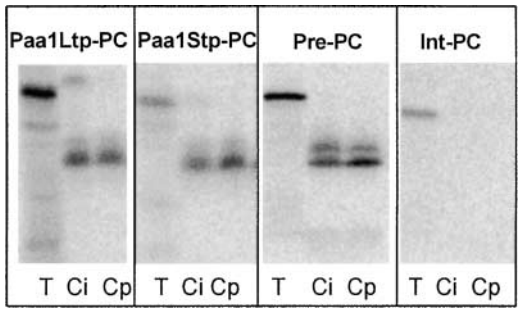

Figure 6. PAA1 Transit Sequence-Dependent Chloroplast Import.

Two versions of the N-terminal sequence of PAA1 were fused with the mature sequence of plastocyanin as a passenger protein. Paa1Ltp-PC (Paa1 long transit peptide fusion) contains 109 amino acids of the PAA1 precursor, including a predicted transit sequence of 104 residues and 5 amino acids of mature PAA1. Paa1Stp-PC (Paa1 short transit peptide fusion) contains 94 amino acids of the PAA1 precursor, including a predicted transit sequence of 89 residues and 5 amino acids of mature PAA1. Paa1Ltp-PC contains 15 additional residues at its N terminus relative to Paa1Stp-PC. Pre-plastocyanin (Pre-PC), the precursor of plastocyanin, and Int-plastocyanin (Int-PC), the precursor of plastocyanin without its transit sequence, served as controls for import and localization. Precursor proteins were labeled by ^{35}S-Met in vitro (T) and incubated with isolated chloroplasts. Chloroplasts were reisolated, and proteins in intact chloroplasts were analyzed either directly (Ci) or after treatment of intact chloroplasts with protease (Cp). Radiolabeled protein bands were visualized using a PhosphorImager after separation by SDS-PAGE.

teins labeled by ^{35}S-Met were synthesized in vitro and incubated with isolated chloroplasts in the light. After import and treatment with protease, the chloroplasts were recovered and fractionated, and radiolabeled proteins were analyzed by SDS-PAGE. The full precursor of plastocyanin and a plastocyanin lacking its chloroplast import domain were used as controls for import and localization.

Both versions of the chimeric protein were imported by chloroplasts with efficiencies comparable to those of the positive control Pre-plastocyanin, and the transit peptides were removed (Figure 6) to produce proteins equal in size to the mature passenger protein. The proteins were resistant to the protease treatment, confirming that they were imported into chloroplasts (Figure 6, Cp). These results indicate that the N-terminal sequence of PAA1 functions as a chloroplast-targeting sequence regardless of which initiation codon is used to start translation. Because proteins that function in the thylakoid membranes or chloroplast inner envelope membrane generally use a cleavable transit sequence for chloroplast import, the results of this import experiment are consistent with PAA1 functioning in either the inner envelope membrane or the thylakoids (Keegstra and Cline, 1999).

Cu Addition Rescues the *paa1* Phenotype

Given the similarity of PAA1 to known Cu-transporting P-type ATPases (Figure 5), we tested the effects of Cu feeding on the phenotypes of *paa1* mutants. Four alleles of *paa1* and their corresponding wild types were cultured on solid agar medium with varying concentrations of $CuSO_4$ (Figure 7). Photosynthetic electron transport activity was estimated from a chlorophyll fluorescence parameter, Φ_{PSII} (the efficiency of PSII photochemistry). Chlorophyll content was used as a second indicator of sensitivity to low or high Cu concentration. On standard agar medium containing 0.1 μM $CuSO_4$ (Murashige and Skoog, 1962), the efficiency of PSII photochemistry was affected severely in *paa1*, consistent with the severe growth-rate phenotype on MS medium (Table 1). Especially in the two alleles in the Col background, *paa1-3* and *paa1-4*, electron transport activity was inhibited almost completely. Chlorophyll content also was reduced drastically in *paa1*. The latter phenotype may be a secondary effect of Cu deficiency in chloroplasts (see below).

Strikingly, both electron transport activity and chlorophyll content were restored completely in the mutants upon the addition of 5 to 10 μM $CuSO_4$ to the growth medium. However, higher concentrations (50 μM) of $CuSO_4$ were toxic to all plant lines. Chlorophyll content was more affected by high Cu levels than was electron transport activity. Seedlings in the Col background were more sensitive to excess $CuSO_4$ than were seedlings in the L*er* background. In both backgrounds, the inhibitory effect of high Cu concentrations was similar for the wild type and *paa1*. The addition of iron (Fe) had no effect on the phenotype of the *paa1* mutants (data not shown). These results indicate that PAA1 plays a role in transporting Cu to a location where it is needed rather than a role in preventing Cu toxicity by sequestering or removing excess Cu.

Cu Content Is Reduced in *paa1* Chloroplasts

To analyze the effect of the *paa1* mutation on metal ion homeostasis more directly, we analyzed transition metal concentrations in shoots and chloroplast fractions (Table 2). We selected this strategy because of the impracticality of performing radioactive Cu uptake experiments with isolated chloroplasts. In wild-type plants, a significant amount of the shoot Cu and Fe was found in the chloroplast, particularly in thylakoids, indicating that this organelle is a major sink in shoots for both elements. Other transition metals (Zn and Mn) were below the detection limit in the chloroplast fractions. Interestingly, whereas the amount of Cu in total shoots was not decreased significantly, there was a 50% reduction for Cu in the total chloroplast fraction of *paa1-1* plants relative to the wild type, and the Cu level was too low to be quantified in the thylakoids of *paa1-1* plants (indicating at least a fourfold reduction relative to the wild type). Fe also was reduced in the *paa1* chloroplasts, but to a much lesser extent.

Although Cu and Fe contents were reduced in the *paa1* chloroplasts, no significant differences were found for the shoot concentrations of these ions (Table 2) or of Zn, S, Ni, and Mo (data not shown). These results indicate that PAA1 does not mediate the delivery of these metal ions from the soil to the shoot and that the *paa1* defect directly affects the Cu content of chloroplasts. Surprisingly, an increase (49% for *paa1-1*) was seen in the shoot concentration of Mn (data not shown).

PAA1 Function Is Required for Holoplastocyanin Formation

Because Cu is an indispensable cofactor of plastocyanin, the photosynthetic electron transport phenotypes of *paa1* mutants

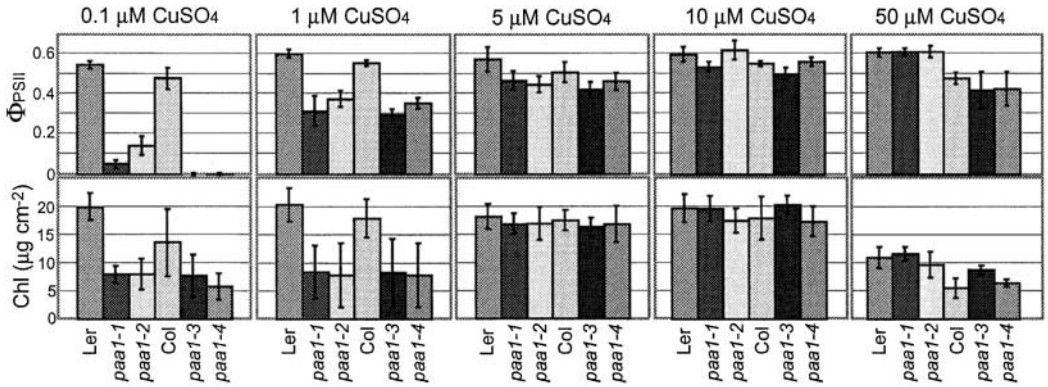

Figure 7. Response of *paa1* Plants to $CuSO_4$.

Four alleles of *paa1* (*paa1-1* to *paa1-4*) and the corresponding wild types were cultured on MS medium supplemented with various concentrations of $CuSO_4$. The standard MS medium contains 0.1 μM $CuSO_4$. The response to Cu was evaluated by a chlorophyll fluorescence parameter, Φ_{PSII} (efficiency of PSII photochemistry) at 200 $\mu mol \cdot m^{-2} \cdot s^{-1}$, and chlorophyll (Chl) content.

might be explained by a lack of functional plastocyanin. To assess this possibility, thylakoid lumen proteins from wild-type and *paa1* plants were subjected to native gel electrophoresis (Li et al., 1990) to separate holoplastocyanin (containing Cu) and apoplastocyanin (lacking Cu). In wild-type plants, plastocyanin was present predominantly in the holo form (Figure 8A, untreated). By contrast, holoplastocyanin was barely detectable in *paa1-1* and *paa1-3*, and apoplastocyanin accumulated instead (Figure 8A, untreated). Treatment with ascorbate and KCN, which converts holoplastocyanin to forms of apoplastocyanin with different electrophoretic mobilities on native gels (Li et al., 1990), indicated that the wild-type plants had much higher contents of plastocyanin polypeptides (Figure 8A, ascorbate/KCN treated), a finding that was confirmed by denaturing SDS-PAGE (Figure 8B). This difference was not apparent in the untreated samples separated on the native gel (Figure 8A, untreated), presumably because the anti-plastocyanin antibody detected apoplastocyanin much more efficiently than holoplastocyanin. The total amount of detectable plastocyanin in the *paa1* mutants (Figure 8B) was much less than that in the wild type, possibly because of the instability of the apoprotein in vivo, as was found in Chlamydomonas (Merchant and Bogorad, 1986; Li and Merchant, 1995). RNA gel blot analysis showed that the transcript levels for plastocyanin were unaffected in *paa1* (data not shown). The lack of holoplastocyanin in *paa1* indicates that insufficient Cu is available in the thylakoid lumen, where holoplastocyanin is assembled (Li et al., 1990).

SOD Isozymes Are Affected in *paa1*

To determine whether PAA1 is likely to be located in the plastid envelope or the thylakoid membranes, we examined the activity and protein level of Cu/ZnSOD, an abundant Cu protein in the chloroplast stroma. Figure 9A shows the activity staining of major SOD isoforms on native gels. SOD isoforms with different metal cofactors can be distinguished by their differential sensitivities to H_2O_2 and KCN (Bowler et al., 1992): Cu/ZnSOD is sensitive to both inhibitors, FeSOD is sensitive to H_2O_2 only, and MnSOD is resistant to both inhibitors. Thus, the SOD activity in the wild type with the lowest mobility corresponds to MnSOD, the SOD with the next lowest mobility corresponds to FeSOD, and the fastest migrating faint doublet represents Cu/ZnSOD activities (Figure 9A). The latter doublet of activities was reported to consist of the cytosolic Cu/ZnSOD isozyme CSD1, which has the higher mobility, and the chloroplastic Cu/ZnSOD, CSD2, with the lower mobility (Kliebenstein et al., 1998). In *paa1*, the activity of Cu/ZnSOD with the lower mobility was undetectable, indicating that the chloroplastic Cu/ZnSOD was affected (Figure 9A). By contrast, the activity of cytosolic Cu/ZnSOD was increased drastically in *paa1* (Figure 9A).

These results may be explained by an impaired Cu supply to the stroma in *paa1*, which in turn would limit the formation of chloroplastic Cu/ZnSOD holoenzyme. Alternatively, the decrease in chloroplastic Cu/ZnSOD activity may be caused by changes in gene expression as a secondary effect of the reduced electron transport in *paa1*. It has been reported that apoCu/ZnSOD is stable (Petrovic et al., 1996); therefore, we could distinguish between the two possibilities by measuring total Cu/ZnSOD polypeptide levels. Figure 9B shows the results of immunoblot analyses of chloroplastic and cytosolic Cu/ZnSOD using specific antibodies raised against CSD2 and CSD1, respectively (Kliebenstein et al., 1998). Although the chloroplastic Cu/ZnSOD

Table 2. Cu and Fe Contents

Genotype	Fraction	Cu	Fe
L*er*	Leaf	10.9 ± 1.5	66.4 ± 8.0
paa1-1	Leaf	9.1 ± 4.6	55.1 ± 9.2
L*er*	Chloroplast	3.4 ± 0.8	45.5 ± 4.1
paa1-1	Chloroplast	1.6 ± 0.2	30.5 ± 3.9
L*er*	Thylakoid	1.8 ± 0.2	26.5 ± 1.5
paa1-1	Thylakoid	< 0.4	16.3 ± 0.4

Values indicate the amount of metal ion (μg) present in fractions (leaf, chloroplast, or thylakoid) corresponding to 1 g of shoot dry weight. Data shown are averages from three measurements.

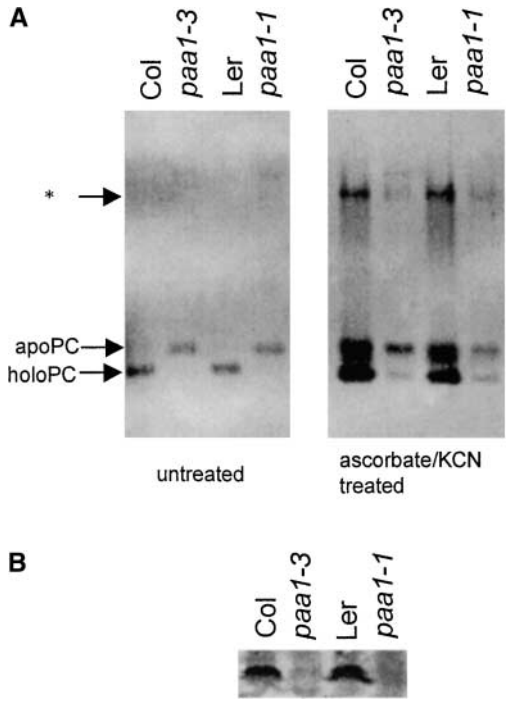

Figure 8. Comparison of Plastocyanin Content in Thylakoids of *paa1* and Wild-Type Plants.

(A) Native PAGE analysis. Thylakoid lumen proteins isolated from rosette leaves of Col, *paa1-3*, L*er*, and *paa1-1* were fractionated on a nondenaturing gel and detected by immunoblot analysis with an antibody against plastocyanin. Samples were analyzed without treatment to assess the mobility of plastocyanin present in the plants (untreated; left gel) or after treatment with ascorbate and KCN to remove possible Cu cofactors (ascorbate/KCN treated; right gel). The band indicated with an asterisk represents a possible oligomer of apoplastocyanin. apoPC, apoplastocyanin; holoPC, holoplastocyanin.

(B) SDS-PAGE and immunodetection of plastocyanin present in thylakoids.

activity was undetectable in *paa1* (Figure 9A), the protein level was significantly higher than in the wild type (Figure 9B, CSD2). The protein level of the cytosolic isoform of Cu/ZnSOD also was higher in *paa1* than in the wild type (Figure 9B, CSD1), consistent with the observed increase in enzyme activity (Figure 9A). RNA gel blot analysis also confirmed the increase of transcripts for both CSD1 and CSD2 (Figure 8C). These results clearly indicate that the decrease in chloroplastic Cu/ZnSOD activity in *paa1* is not caused by the downregulation of CSD2 gene expression. We conclude that chloroplastic Cu/ZnSOD accumulates in the inactive apoprotein form in *paa1* mutants as a result of insufficient Cu delivery to the stroma.

Surprisingly, chloroplastic FeSOD activity also was impaired severely in *paa1* (Figure 9A), although mitochondrial MnSOD activity was not affected. By analogy with the Cu-dependent uptake of Fe by yeast cells (Askwith et al., 1994; Dancis et al., 1994; Yuan et al., 1995), the reduced FeSOD activity could be attributable to impaired Fe uptake by Cu-deficient *paa1* chloroplasts or to downregulation of its expression. To assess the latter possibility, we compared the polypeptide and mRNA levels in *paa1* and wild-type plants. The FeSOD protein level was affected severely in *paa1* (Figure 9B). Furthermore, RNA gel blot analysis revealed a drastic reduction of FeSOD transcript levels in *paa1* (Figure 8C). Therefore, the decrease in the activity of chloroplastic FeSOD in *paa1* was caused by a downregulation of FeSOD gene expression, possibly as a secondary effect of the impaired photosynthetic electron transport. Direct measurement of Fe in chloroplasts indicated some reduction of Fe content in *paa1* chloroplasts (Table 2), which, along with the reduced chlorophyll content, could have been a secondary effect of Cu deficiency. Consistent with this hypothesis, we observed that the level of a major Fe protein, cytochrome *f*, was similar in *paa1* and the wild type, and the overall polypeptide profiles of *paa1* and wild-type chloroplasts were very similar (data not shown).

DISCUSSION

PAA1 Encodes a Chloroplast-Localized P-Type ATPase Required for the Function of Chloroplast Cu Proteins

PAA1 was discovered as an Arabidopsis homolog of the cyanobacterial Cu-transporting P-type ATPase PacS (Kanamaru et al., 1994; Tabata et al., 1997). We have determined that PAA1 contains a functional chloroplast-targeting sequence (Figure 6). Although the presence of functional plastid-targeting

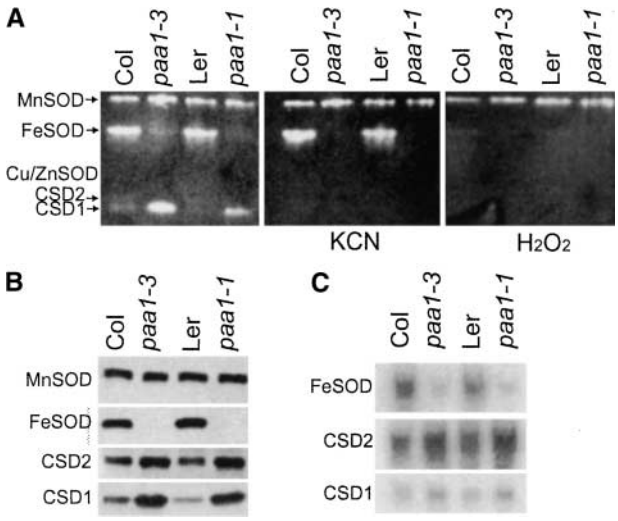

Figure 9. Analysis of Other Metalloproteins in *paa1*.

(A) Gel assay for the activity of the major SOD isozymes. Total soluble proteins isolated from rosette leaves of Col, *paa1-3*, L*er*, and *paa1-1* were fractionated on a nondenaturing gel and stained for SOD activity. Gels were preincubated with KCN, which inhibits Cu/ZnSOD, or H_2O_2, which inhibits both Cu/ZnSOD and FeSOD, to distinguish their activities.

(B) Determination of protein levels of SOD isoforms. Proteins isolated from rosette leaves were fractionated by SDS-PAGE, and each SOD isoform was detected by immunoblot analysis using a specific antibody.

(C) Determination of transcript levels of SOD isoforms. Total RNA isolated from rosette leaves was fractionated by agarose gel electrophoresis and detected with probes specific for CSD1, CSD2, and FSD.

information does not exclude the possibility that, besides plastids, PAA1 could be targeted to another organelle, as has been reported for some proteins (Duchene et al., 2001), such cases are rare, and we consider such dual targeting very unlikely in view of the phenotypes of *paa1* mutants. We have characterized the function of *PAA1* in Arabidopsis by analyzing the phenotypes of six mutant alleles in the gene. Alleles of *PAA1* were identified by their high-chlorophyll-fluorescence phenotype (Figure 1) caused by a decrease in photosynthetic electron transport (Figure 2). This mutant phenotype can be explained by an impaired transport of Cu into chloroplasts, which results in insufficient active holoplastocyanin formation (Figure 8). Consistent with the phenotype in electron transport (Figure 7), holoplastocyanin levels were complemented partially by Cu supplementation (S. Abdel-Ghany and M. Pilon, unpublished data). However, the addition of the Cu chelator cuprizone (1 μM) did not affect the holoplastocyanin level further. PAA1 also was involved in Cu ion delivery to the stromal Cu/ZnSOD isozyme (Figure 9). The *paa1* mutants accumulated increased levels of this protein, presumably the apoprotein form, which lacked detectable activity. The decreases in plastocyanin and Cu/ZnSOD activities were paralleled by a decrease in the Cu content of *paa1* chloroplasts but not leaves (Table 2).

Based on these observations, we propose that PAA1 is located in the plastid inner envelope membrane and that it transports Cu across the plastid envelope. Probably, PAA1 donates Cu to a stromal metallochaperone for chloroplast Cu/ZnSOD or to a chaperone such as cyanobacterial ATX1 (Tottey et al., 2002) that can target Cu to thylakoid membranes. To reach plastocyanin, the Cu ion must be pumped across the thylakoid membrane into the lumen. Indeed, we have identified mutants similar to *paa1* that affect another putative Cu-transporting P-type ATPase (*PAA2*/At5g21930), which also has a predicted plastid-targeting signal (our unpublished data). *PAA2* appears to encode a functional homolog of cyanobacterial PacS, which is located in thylakoid membranes (Kanamaru et al., 1994). PAA1 is more similar to CtaA, the proposed Cu transporter in the cytoplasmic membrane of cyanobacteria, than to PacS, and the converse is true for PAA2. Considering the endosymbiotic origin of chloroplasts, these similarities support the location of PAA1 in the chloroplast envelope. Another possible Cu-transporting P-type ATPase (*HMA5*/At1g63440) possesses a putative targeting signal to mitochondria and possibly functions in Cu delivery to mitochondrial proteins such as cytochrome *c* oxidase.

We have made several attempts to determine more directly the location of the PAA1 protein in plant cells, but to date we have been unsuccessful. We have raised several antisera against PAA1 domains, but these antisera failed to detect PAA1 in extracts of plants or chloroplasts, probably because the expression level of PAA1 is very low. Only two ESTs for *PAA1* are present in the GenBank database (February 2003). Transgenic expression of an epitope-tagged version of PAA1 in a *paa1* mutant background also was unsuccessful.

Effects of *paa1* Mutations

In view of the important roles of Cu enzymes in photosynthesis, it is somewhat surprising that *paa1*, with such impaired Cu metabolism in the chloroplasts and much reduced activities of two major Cu proteins, still manages to survive, at least under laboratory conditions. Despite a severe lack of functional plastocyanin, the maximum ETR was decreased only to 30% of the wild-type level in *paa1* mutants grown in soil (Figure 2). Residual ETR in *paa1* likely is attributable in part to the activity of a constitutively expressed cytochrome c_6 in the thylakoid lumen that has functional overlap with plastocyanin (Gupta et al., 2002). Consistent with this hypothesis, the growth defect of *paa1* mutants that we observed (Figure 1, Table 1) is similar to that of transgenic Arabidopsis plants that lack detectable plastocyanin as a result of the expression of a plastocyanin RNA interference construct (Gupta et al., 2002). When the *paa1* alleles in the Col background (*paa1-3* and *paa1-4*) were cultured on medium containing only 0.1 μM $CuSO_4$, electron transport was arrested almost completely (Figure 7). In alleles in the L*er* background (*paa1-1* and *paa1-2*), however, the phenotype was significantly milder (Figure 7), despite very similar defects in plastocyanin. This difference in phenotype between the Col and L*er* backgrounds may be attributable to a higher level of cytochrome c_6 expression in L*er* compared with Col. Despite the existence of cytochrome c_6, the defects in photosynthesis in plants without plastocyanin (Gupta et al., 2002) and the pleiotropic defects associated with the *paa1* mutations (see below) make it very unlikely that such plants grow and compete under natural conditions.

In contrast to the divergent phenotypes observed for *ran1* alleles (Hirayama et al., 1999; Woeste and Kieber, 2000), the phenotypes of the six *paa1* alleles are rather uniform, although they are affected by the strain background (Figures 2 and 7). The uniform phenotypes of *paa1* alleles relate to the fact that electron transport is affected only when plastocyanin levels are reduced drastically. In our screening system, we monitored electron transport; therefore, only strong alleles of *paa1* were identified. In this context, it is worth mentioning that the weak alleles, *ran1-1* and *ran1-2*, and the strong allele, *ran1-3*, were identified by different screening strategies (Hirayama et al., 1999; Woeste and Kieber, 2000).

We observed an unexpected decrease in chloroplastic FeSOD activity and protein level in *paa1* (Figure 9). The decrease in FeSOD activity was the result of a change in gene expression and not decreased Fe availability. In wild-type plants, the expression of FeSOD is enhanced by adding methyl viologen, an effect that is reversed by adding the PSII inhibitor DCMU (Tsang et al., 1991). These observations suggest that the expression of FeSOD is controlled by active oxygen species generated by oxygen reduction (water-water cycle) at the acceptor side of PSI (Asada, 1999). Given the fact that electron transport between the two photosystems is restricted in *paa1* (Figure 3), the rate of oxygen reduction at PSI should be decreased. This effect could lead to the observed depression of FeSOD expression.

In contrast to chloroplastic FeSOD, the transcript and peptide levels of both chloroplastic and cytosolic Cu/ZnSOD were increased. Coregulation of chloroplastic and cytosolic Cu/ZnSOD by LSD1 has been shown previously in response to salicylic acid (Kliebenstein et al., 1999). Decreased levels of FeSOD typically are linked with increased Cu/ZnSOD (both plastidic and cytosolic) and vice versa (Kliebenstein, 1999).

There are several possible explanations for this reciprocal regulation of SOD isozymes. First, the defect in photosynthetic electron transport in *paa1* might have initiated a signal that leads to the increased expression of cytosolic Cu/ZnSOD activity. Although the limitation of electron transport at plastocyanin would diminish oxygen reduction at the acceptor side of PSI, the upstream electron transport pathway was more reduced by electrons (Figure 3). It is possible that the overreduction of the plastoquinone pool or electron carriers in the cytochrome b_6f complex might generate a signal related to the PSII excitation pressure (Escoubas et al., 1995), which could enhance both cytosolic and chloroplastic Cu/ZnSOD expression. Second, chloroplast Cu proteins, especially plastocyanin, constitute a major sink for Cu in green tissue. In the absence of efficient Cu transport to the chloroplasts, cytosolic Cu/ZnSOD might serve as a sink for the extra available Cu in the cytosol. In yeast and humans, apoCu/ZnSOD functions to absorb excess Cu and to buffer the Cu concentration in cells (Culotta et al., 1995; Petrovic et al., 1996). Third, increased expression of cytosolic Cu/ZnSOD might be induced in response to reactive oxygen species that are generated by the presence of excess Cu in the cytosol. Cu supplementation restored some chloroplastic Cu/ZnSOD activity in *paa1*. When grown with the Cu chelator cuprizone (1 μM), both the wild type and *paa1* exhibited the same SOD activity profile (S. Abdel-Ghany and M. Pilon, unpublished results).

Compared with the wild type, *paa1* also exhibited a reduction in chlorophyll content when grown on medium containing low Cu (0.1 μM $CuSO_4$; Figure 7). The loss of chlorophyll could be explained by the impaired activity of both Cu/ZnSOD and Fe-SOD in *paa1* chloroplasts. These enzymes provide protection from oxidative stress by scavenging superoxide, thus preventing the formation of highly reactive hydroxyl radicals. With insufficient SOD activity present in chloroplasts, bleaching of chlorophyll might be expected even at low light intensities.

Direct measurement of Fe in chloroplasts indicated some reduction in the Fe content of *paa1* chloroplasts (Table 2). In sugar beet, cytochrome *f* activity is diminished under Fe deficiency to the same extent as chlorophyll activity (Spiller and Terry, 1980), and Fe deficiency greatly affects the abundance and composition of the thylakoid membranes (Spiller and Terry, 1980; Terry, 1980). In Chlamydomonas, Fe deficiency also leads to a reduction in cytochrome *f* polypeptide levels and to severe downregulation and remodeling of PSI, which may be mediated by an effect of Fe on chlorophyll synthesis (Moseley et al., 2002). The phenotypes observed for *paa1* (mild reduction in chlorophyll and severe reduction in electron transport) were more similar to the effects of Cu deficiency observed in sugar beet (Droppa et al., 1984) but were distinct from the effects of Fe deficiency described above.

Cu Homeostasis in Chloroplasts

The *paa1* phenotype was rescued by the addition of extra Cu to the growth medium even in what seems to be a null allele, *paa1-1* (Figure 7). This finding suggests that Cu can be incorporated into chloroplasts via an alternative pathway, perhaps by means of a low-affinity transporter with broad metal specificity. However, the efficiency of this alternative transport system seems much lower than that of the PAA1 pathway, because full restoration of electron transport required the plants to be grown at high Cu concentrations (~10 μM) that are very close to the toxic range (Figure 7).

A proposed function of P-type ATPases besides their role in ion acquisition and delivery is the extrusion of toxic ions from the cytosol; therefore, we must consider this possibility for PAA1 as well. In cyanobacteria, two Cu-transporting P-type ATPases that function in plastocyanin biogenesis are present: PacS and CtaA (Tottey et al., 2001). The presence of high Cu enhanced *pacS* expression, and a *pacS* knockout mutant exhibited greater sensitivity to Cu ions (Kanamaru et al., 1994; Tottey et al., 2001). Thus, an additional role for PacS in Cu homeostasis seems to be the extrusion of Cu from the cyanobacterial cytosol, preventing the accumulation of toxic Cu levels in the cell (Kanamaru et al., 1994). PacS localizes in thylakoid membranes and therefore may pump excess Cu into the thylakoid lumen (Kanamaru et al., 1994). By contrast, cyanobacterial mutants defective in CtaA, which presumably localizes to the cyanobacterial cytoplasmic membrane, are not more sensitive to high Cu but instead display a Cu-deficiency phenotype (Tottey et al., 2001). Thus, CtaA may play a role mainly in Cu acquisition. Although PAA1 was identified originally as a homolog of PacS (Tabata et al., 1997), its predicted amino acid sequence is more similar to that of CtaA. Like *ctaA* mutants in cyanobacteria, *paa1* chloroplasts are deficient in Cu, and photosynthesis is not hypersensitive to excess supplied Cu. Therefore, we consider Arabidopsis PAA1 to be a functional homolog of cyanobacterial CtaA.

METHODS

Plant Materials and Growth Conditions

The background of *Arabidopsis thaliana paa1-1* and *paa1-2* is Landsberg *erecta*, and that of *paa1-4* and *paa1-6* is Columbia *gl1* (Col-3). The *paa1-3* and *paa1-5* alleles (Col-0 background) were obtained by independent screening (Niyogi et al., 1998). All alleles were derived by mutagenesis with ethyl methanesulfonate with the exception of *paa1-3*, which was mutagenized by fast-neutron bombardment.

Plants were grown in Metromix potting soil (Scotts, Hope, AR) under controlled conditions (light intensity of 40 $\mu mol \cdot m^{-2} \cdot s^{-1}$ in a 16-h/8-h light/dark cycle at 23°C). For chloroplast isolation and extraction of plastocyanin, larger numbers of plants were grown in a greenhouse with natural sunlight supplemented by lighting from sodium lamps to give 15 h of light during the photoperiod. Seeds used for the analyses shown in Table 1 and Figure 7 were surface-sterilized and sown on agar-solidified MS medium containing 1% sucrose (Murashige and Skoog, 1962). The medium was supplemented with $CuSO_4$ as indicated in Figure 7.

Map-Based Cloning

The *paa1-1* mutation was mapped with cleaved amplified polymorphic sequence markers (Konieczny and Ausubel, 1993) and simple sequence length polymorphism markers (Bell and Ecker, 1994). Genomic DNA was isolated from F2 plants derived from the cross between *paa1-1* and the polymorphic wild type (Col). Genomic *PAA1* sequences containing the wild type and all *paa1* alleles were amplified by PCR using Ex-Taq DNA polymerase (Takara, Kyoto, Japan). Resulting PCR products were se-

quenced directly using a dye terminator cycle sequencing kit and an ABI Prism 377 sequencer (Perkin-Elmer, Norwalk, CT).

For complementation of the *paa1* mutation, the wild-type *PAA1* sequence was amplified from BAC clone F17M5 using primers 5′-GGAATCTTCCGTCgaCTATTGG-3′ and 5′-GAACAAGACCCgGATCcAACTAC-3′ (lowercase letters indicate mismatches introduced to create restriction sites). The PCR product was subcloned in pBI101. The resulting plasmid was introduced into the *Agrobacterium tumefaciens* pMP40 strain and then transformed (Clough and Bent, 1998) into *paa1-3*.

Chlorophyll Fluorescence Analysis

Chlorophyll fluorescence was measured with a pulse-amplitude modulation (PAM) fluorometer (Walz, Effeltrich, Germany) with an ED101 emitter-detector unit as described (Schreiber et al., 1986). The minimum fluorescence at open photosystem II (PSII) centers in the dark-adapted state (Fo) was excited by a weak measuring light (650 nm) at a light intensity of 0.05 to 0.1 $\mu mol \cdot m^{-2} \cdot s^{-1}$. A saturating pulse of white light (800 ms, 3000 $\mu mol \cdot m^{-2} \cdot s^{-1}$) was applied to determine the maximum fluorescence at closed PSII centers in the dark-adapted state (Fm) and during actinic light illumination (Fm′). The steady state fluorescence level (Fs) was recorded during actinic light illumination (15 to 1000 $\mu mol \cdot m^{-2} \cdot s^{-1}$). The minimum fluorescence in the light-adapted state (Fo′) was measured in the presence of far-red light after the actinic light was turned off. Nonphotochemical quenching was calculated as (Fm − Fm′)/Fm′. The light-intensity dependence of steady state fluorescence parameters was measured using a MINI-PAM portable chlorophyll fluorometer (Walz). The quantum yield of PSII (Φ_{PSII}) was calculated as (Fm′ − Fs)/Fm′ (Genty et al., 1989). The relative rate of electron transport through PSII (electron transport rate) was calculated as $\Phi_{PSII} \times$ PFD. The reduction state of the quinone acceptor of PSII (1 − qP) was calculated as (Fs − Fo′)/(Fm′ − Fo′).

Measurement of the Redox State of P700

Redox changes in P700 were assessed by monitoring the A_{820} with a PAM chlorophyll fluorometer with an ED800T emitter-detector unit as described (Schreiber et al., 1988). The reduction state of P700 was calculated as 1 − (ΔA/ΔAmax). In vivo $P700^+$ was recorded during actinic light illumination as ΔA_{820}. The maximum in vivo content of $P700^+$ (ΔAmax) was estimated by the absorbance change induced by far-red light illumination (720 nm, 0.66 $\mu mol \cdot m^{-2} \cdot s^{-1}$).

Chlorophyll Content Determination

Chlorophyll content was determined by absorbance changes in intact leaves using SPAD-502 (Minolta, Osaka, Japan). The data were standardized by the conventional method (Bruinsma, 1961).

In Vitro Chloroplast Import Assay

The transit sequence region of *PAA1* was amplified by PCR using either of two forward primers (5′-gggggtaccGATAACGGGACTCGAGAGATTGAG-3′ for the long fusion and 5′-gggggtacctTGGAGTCTACACTCTCAGCTTTCT-3′ for the short fusion) in combination with a reverse primer (5′-ggggtccatggATCCAGAACCGCCGCCACTTGA-3′) (lowercase letters indicate mismatches introduced to create restriction sites and to disrupt the first initiation codon in the short fusion). The PCR products were digested with KpnI and NcoI and ligated with the aid of a linker (5′-AGCTGTAC-3′) into a HindIII- and NcoI-digested pSPPC74 vector, which contains the plastocyanin sequence from *Silene pratensis* as a passenger protein (Smeekens et al., 1986). The resulting plasmids were linearized with PvuII and transcribed in vitro using SP6 polymerase (Epicenter Technologies, Madison, WI) according to the manufacturer's instructions. Radiolabeled precursors were synthesized in a wheat germ lysate system in the presence of ^{35}S-Met (specific activity of 1300 Ci/mmol; Amersham/Pharmacia, Piscataway NJ) according to suggested protocols (Promega, Madison, WI).

Chloroplasts for import experiments were isolated from 10-day-old pea seedlings (cv Little Marvel) and incubated with radiolabeled precursors as described (Pilon et al., 1992). The postimport thermolysin treatment, reisolation of intact chloroplasts through 40% Percoll cushions, and fractionation into the stroma and membrane fractions were performed essentially as described (Smeekens et al., 1986). The proteins in fractions from import experiments equivalent to 10 μg of chlorophyll were separated by SDS-PAGE (15% gel). The gel was fixed and dried, and radiolabeled proteins were visualized and quantified using a STORM PhosphorImager (Molecular Dynamics, Sunnyvale, CA). The clones encoding the control proteins Pre-plastocyanin and Int-plastocyanin have been described (Smeekens et al., 1986).

Isolation of Arabidopsis Chloroplasts and Separation of Apoplastocyanin and Holoplastocyanin

To analyze the relative amounts of apoplastocyanin and holoplastocyanin, intact chloroplasts were isolated from rosette leaves of plants (3 to 4 weeks old) as described by Rensink et al. (1998). The intactness of chloroplast preparations was confirmed by comparing the abundance of the stromal protein, AtCpNifS (Pilon-Smits et al., 2002), relative to chlorophyll in homogenate and isolated chloroplasts. Chloroplasts equivalent to 100 μg of chlorophyll were precipitated and then lysed by resuspension in 300 μL of 10 mM Tris-HCl, pH 8. After 2 min on ice, an equal volume of 660 mM sorbitol and 100 mM Hepes-KOH, pH 8, was added. The thylakoid membranes were precipitated by centrifugation and resuspended in 330 mM sorbitol and 50 mM Hepes-KOH, pH 8. Lumen proteins were isolated and the presence of the Cu cofactor in plastocyanin was analyzed essentially as described by Li et al. (1990). Aliquots of the samples were incubated in 2.5 mM ascorbate on ice for 5 min and then in 10 mM KCN on ice for an additional 5 min to remove the Cu cofactor from plastocyanin. Proteins were separated by native 15% PAGE and then blotted to a nitrocellulose membrane. Immunodetection of holoplastocyanin and apoplastocyanin was performed using a plastocyanin-specific antiserum (de Boer et al., 1988).

Metal Ion Measurements

Plants were grown on soil for 4 weeks. Approximately 5 g of shoots was washed three times for 5 min with distilled water, drained, and dried overnight at 70°C. Four 50-mg aliquots of dried plant material were acid digested for 6 h at 130°C in 0.5 mL of concentrated nitric acid. Intact chloroplasts and thylakoids were isolated from 25 g of shoots as described above. Measurements of dry weight and chlorophyll content indicated that 1 g of dry weight corresponded to 8 mg of chlorophyll. Chloroplast fractions corresponding to 0.4 mg of chlorophyll were pelleted and dissolved in water. The fractions were dried in a clean glass tube and digested with 0.5 mL of concentrated nitric acid. After digestion, the samples were diluted to 5 mL with distilled water. Fifty microliters of each sample was diluted again with 9 volumes of water and used for metal ion analysis on a Dionex ion chromatography system (Sunnyvale, CA). Samples with low amounts of transition metals were dried by heating and redissolved in 1 mL of 1% nitric acid, which was used directly for analysis by ion chromatography. The Dionex ion chromatography system consisted of a GP50 pump, an AS40 autosampler and injector with a 100-μL loop size, an IonPac CS5A column, a PC10 postcolumn delivery pump, and a UVD170 detector, all controlled by Chromeleon software. The eluent was 7 mM pyridine-2,6-dicarboxylic acid, 66 mM potassium hydroxide, 5.6 mM potassium phosphate, and 74 mM formic

acid, pH 4.2, and the flow rate was 1.2 mL/min. Postcolumn reagent [60 mg/L 4-(2-pyridylazo)-resorcinol in 1 M 2-dimethylaminoethanol, 0.5 M ammonium hydroxide, and 0.3 M sodium bicarbonate, pH 10.4] was supplied at 0.4 mL/min.

Transition metal ions were detected by absorption at 530 nm after postcolumn complex formation with the 4-(2-pyridylazo)-resorcinol reagent. Metal ions (Fe, Cu, Ni, Zn, Co, Cd, and Mn) were identified by retention times and quantified by peak area integration using standards of known concentration. The detection limits were 0.4 ng for Fe, Cu, and Zn and 1 ng for Mn (which translates into a detection limit of 0.4 μg/g dry weight for Fe and Cu in our measurements presented in Table 2). The shoot samples also were analyzed by inductively coupled plasma–atomic emission spectroscopy (Colorado State University Soil Science Laboratory), which gave comparable results for the transition metals and had the advantage of being able to measure additional elements, but this method was not sensitive enough to measure transition metals other than Fe in the chloroplast fractions.

Superoxide Dismutase Activity Gels

Rosette leaves (0.2 g) were harvested and frozen immediately in liquid nitrogen. Samples were prepared as described by Bowler et al. (1989) except that the potassium phosphate buffer had a pH of 7.4. The protein concentrations were quantified using the Bio-Rad protein assay (Hercules, CA). Thirty micrograms of total soluble protein was subjected to electrophoresis at 120 V for 2 h on a 12% acrylamide nondenaturing gel. The gel was stained for superoxide dismutase (SOD) activity as described by Beauchamp and Fridovich (1971). The SOD isozymes were identified by differential inhibition using 2 mM KCN to inhibit Cu/ZnSOD (Van Camp et al., 1996) or 3 mM H_2O_2 to inhibit Cu/ZnSOD and FeSOD.

Immunoblot Analysis

Rosette leaves were harvested and frozen immediately in liquid nitrogen. For the cytochrome *f* blots, thylakoids were isolated by grinding frozen leaves in grinding buffer (0.33 M glucose, 50 mM Hepes-KOH, pH 7.5, 0.4 M NaCl, 2 mM $MgCl_2$, 1 mM EDTA, 2 mg/mL BSA, 1 mM aminobenzyamidine, 1 mM aminocaproic acid, and 100 μM phenylmethylsulfonyl fluoride) followed by centrifugation at 500 rpm to pellet cell debris. The supernatant was centrifuged at 3,500 rpm for 10 min, and the pellet was resuspended in wash buffer (50 mM Hepes-KOH, pH 7.5, 0.15 M NaCl, 4 mM $MgCl_2$, 1 mM EDTA, 1 mM aminobenzyamidine, 1 mM aminocaproic acid, and 100 μM phenylmethylsulfonyl fluoride) and pelleted again at 10,000 rpm for 5 min. The pellet was washed a total of three times before it was resuspended in a small amount of wash buffer. For SOD isozymes, the extracts prepared for the activity gels were used. Protein concentrations in the thylakoid samples and in the SOD extracts were determined using the Bio-Rad protein assay. Thylakoids and SOD extracts were solubilized in solubilization buffer (250 mM Tris-HCl, pH 6.8, 3.5% SDS, 10% [v/v] glycerol, 1 M urea, and 10% [v/v] β-mercaptoethanol). Ten micrograms of protein was loaded onto a precast gel (10 to 20% gradient) with Tris-glycine buffer (Novex, San Diego, CA), and SDS-PAGE was performed under denaturing conditions. Proteins were blotted onto a polyvinylidene difluoride membrane and detected using the enhanced chemiluminescence protein gel blot kit from Amersham Pharmacia Biotech (Piscataway, NJ). The anti-cytochrome *f* antibody was provided by Richard Malkin (University of California, Berkeley). SOD isoforms were detected using specific antibodies (Kliebenstein et al., 1998).

RNA Gel Blot Analysis

Total RNA was isolated from rosette leaves and subjected to RNA gel blot analysis essentially as described (Sambrook et al., 1989). The ^{32}P-labeled probes were obtained by PCR amplification using the following oligonucleotide pairs: 5′-GAGTTGCAGTTTTGAACAGC-3′ and 5′-TTCTTTGGAAACGTAGCAGC-3′ (CSD1), 5′-AAACGTCAAACATAGCAGCAG-3′ and 5′-AGTAAACACATCACTGTCAT-3′ (CSD2), and 5′-CAAACTCTGGAGTTTCACTG-3′ and 5′-TCAAGTCTGGCACTTACAGC-3′ (FSD).

Upon request, all novel materials described in this article will be made available in a timely manner for noncommercial research purposes.

ACKNOWLEDGMENTS

We thank Momoko Miyata and Alba Phippard for their excellent technical assistance. We are grateful to Richard Malkin, Daniel Kliebenstein, Robert Last, and Patricia Conklin for the generous antibody gifts. We also thank Masao Tasaka, Takeshi Mizuno, Jun-ichi Mano, and Daniel Kliebenstein for their valuable suggestions. The BAC clone was obtained from the ABRC. This work was supported by grants from the Research for the Future Program from the Japan Society for the Promotion of Science (JSPS-RFTF96R16001 and JSPS-RFTF00L01604) to T.S., from the U.S. Department of Agriculture National Research Initiative (98-35306-6600) and the Searle Scholars Program/The Chicago Community Trust to K.K.N., and from the U.S. National Science Foundation (MCB-0091163) to M.P.

Received March 11, 2003; accepted April 1, 2003.

REFERENCES

America, T., Hageman, J., Guera, A., Rook, F., Archer, K., Keegstra, K., and Weisbeek, P. (1994). Methotrexate does not block import of a DHFR fusion protein into chloroplasts. Plant Mol. Biol. **24,** 283–294.

Asada, K. (1999). The water-water cycle in chloroplasts: Scavenging of active oxygens and dissipation of excess photons. Annu. Rev. Plant Physiol. Plant Mol. Biol. **50,** 601–639.

Askwith, C., Eide, D., Van Ho, A., Bernard, P.S., Li, L., Davis-Kaplan, S., Sipe, D.M., and Kaplan, J. (1994). The *FET3* gene of *S. cerevisiae* encodes a multicopper oxidase required for ferrous iron uptake. Cell **76,** 403–410.

Axelsen, K.B., and Palmgren, M.G. (2001). Inventory of the superfamily of P-type ion pumps in Arabidopsis. Plant Physiol. **126,** 696–706.

Beauchamp, C., and Fridovich, I. (1971). Superoxide dismutase: Improved assays and an assay applicable to acrylamide gels. Anal. Biochem. **44,** 276–287.

Bell, C.J., and Ecker, J.R. (1994). Assignment of 30 microsatellite loci to the linkage map of Arabidopsis. Genomics **19,** 137–144.

Bowler, C., Alliotte, T., De Loose, M., Van Montagu, M., and Inzé, D. (1989). The induction of manganese superoxide dismutase in response to stress in *Nicotiana plumbaginifolia*. EMBO J. **8,** 31–38.

Bowler, C., Van Camp, W., Van Montagu, M., and Inzé, D. (1994). Superoxide dismutase in plants. Crit. Rev. Plant Sci. **13,** 199–218.

Bowler, C., Van Montagu, M., and Inzé, D. (1992). Superoxide dismutase and stress tolerance. Annu. Rev. Plant Physiol. Plant Mol. Biol. **43,** 83–116.

Bruinsma, J. (1961). A comment on the spectrophotometric determination of chlorophyll. Biochim. Biophys. Acta **52,** 576–578.

Clough, S.J., and Bent, A.F. (1998). Floral dip: A simplified method for *Agrobacterium*-mediated transformation of *Arabidopsis thaliana*. Plant J. **16,** 735–743.

Culotta, V.C., Joh, H.-D., Lin, S.-J., Slekar, K.H., and Strain, J. (1995). A physiological role for *Saccharomyces cerevisiae* copper/zinc superoxide dismutase in copper buffering. J. Biol. Chem. **270,** 29991–29997.

Dancis, A., Yuan, D.S., Haile, D., Askwith, C., Eide, D., Moehle, C., Kaplan, J., and Klausner, R.D. (1994). Molecular characterization of

a copper transport protein in *S. cerevisiae*: An unexpected role for copper in iron transport. Cell **76,** 393–402.

de Boer, D., Cremers, R., Teertstra, L., Smits, L., Hille, J., Smeekens, S., and Weisbeek, P. (1988). In vivo import of plastocyanin and a fusion protein into developmentally different plastids of transgenic plants. EMBO J. **7,** 2631–2635.

Droppa, M., Terry, N., and Horvath, G. (1984). Effects of Cu deficiency on photosynthetic electron transport. Proc. Natl. Acad. Sci. USA **81,** 2369–2373.

Duchene, A.M., Peeters, N., Dietrich, A., Cosset, A., Small, I.D., and Wintz, H. (2001). Overlapping destinations for two dual targeted glycyl-tRNA synthetases in *Arabidopsis thaliana* and *Phaseolus vulgaris*. J. Biol. Chem. **276,** 15275–15283.

Escoubas, J.-M., Lomas, M., LaRoche, J., and Falkowski, P.G. (1995). Light intensity regulation of *cab* gene transcription is signaled by the redox state of the plastoquinone pool. Proc. Natl. Acad. Sci. USA **92,** 10237–10241.

Ferguson-Miller, S., and Babcock, G.T. (1996). Heme/copper terminal oxidases. Chem. Rev. **96,** 2889–2907.

Fox, T.C., and Guerinot, M.L. (1998). Molecular biology of cation transport in plants. Annu. Rev. Plant Physiol. Plant Mol. Biol. **49,** 669–696.

Genty, B., Briantais, J.-M., and Baker, N.R. (1989). The relationship between quantum yield of photosynthetic electron transport and quenching of chlorophyll fluorescence. Biochim. Biophys. Acta **990,** 87–92.

Guera, A., America, T., van Waas, M., and Weisbeek, P.J. (1993). A strong protein unfolding activity is associated with the binding of precursor chloroplast proteins to chloroplast envelopes. Plant Mol. Biol. **23,** 309–324.

Gupta, R., He, Z., and Luan, S. (2002). Functional relationship of Arabidopsis cytochrome c_6 and plastocyanin in photosynthetic electron transport. Nature **417,** 567–571.

Himelblau, E., and Amasino, R.M. (2000). Delivering copper within plant cells. Curr. Opin. Plant Biol. **3,** 205–210.

Himelblau, E., Mira, H., Lin, S.-J., Culotta, V.C., Penarrubia, L., and Amasino, R.M. (1998). Identification of a functional homolog of the yeast copper homeostasis gene *ATX1* from Arabidopsis. Plant Physiol. **117,** 1227–1234.

Hirayama, T., Kieber, J.J., Hirayama, N., Kogan, M., Guzman, P., Nourizadeh, S., Alonso, J.M., Dailey, W.P., Dancis, A., and Ecker, J.R. (1999). RESPONSIVE-TO-ANTAGONIST1, a Menkes/Wilson disease-related copper transporter, is required for ethylene signaling in Arabidopsis. Cell **97,** 383–393.

Kampfenkel, K., Kushnir, S., Babichuk, E., Inzé, D., and Van Montagu, M. (1995). Molecular characterization of a putative *Arabidopsis thaliana* copper transporter and its yeast homologue. J. Biol. Chem. **270,** 28479–28486.

Kanamaru, K., Kashiwagi, S., and Mizuno, T. (1994). A copper-transporting P-type ATPase found in the thylakoid membrane of the cyanobacterium *Synechococcus* species PCC7942. Mol. Microbiol. **13,** 369–377.

Keegstra, K., and Cline, K. (1999). Protein import and routing systems of chloroplasts. Plant Cell **11,** 557–570.

Kieselbach, T., Hagman, A., Andersson, B., and Schroder, W.P. (1998). The thylakoid lumen of chloroplasts: Isolation and characterization. J. Biol. Chem. **273,** 6710–6716.

Kliebenstein, D.J. (1999). Arabidopsis Superoxide Dismutase. Master's thesis (Ithaca, NY: Cornell University).

Kliebenstein, D.J., Dietrich, R.A., Martin, A.C., Last, R.L., and Dangl, J.L. (1999). LSD1 regulates salicylic acid induction of copper zinc superoxide dismutase in *Arabidopsis thaliana*. Mol. Plant-Microbe Interact. **12,** 1022–1026.

Kliebenstein, D.J., Monde, R.-A., and Last, R.L. (1998). Superoxide dismutase in Arabidopsis: An eclectic enzyme family with disparate regulation and protein localization. Plant Physiol. **118,** 637–650.

Konieczny, A., and Ausubel, F.M. (1993). A procedure for mapping *Arabidopsis* mutations using co-dominant ecotype-specific PCR-based markers. Plant J. **4,** 403–410.

Li, H.H., and Merchant, S. (1995). Degradation of plastocyanin in copper-deficient *Chlamydomonas reinhardtii*: Evidence for a protease-susceptible conformation of the apoprotein and regulated proteolysis. J. Biol. Chem. **270,** 23504–23510.

Li, H.H., Quinn, J., Culler, D., Girard-Bascou, J., and Merchant, S. (1996). Molecular genetic analysis of plastocyanin biosynthesis in *Chlamydomonas reinhardtii*. J. Biol. Chem. **271,** 31283–31289.

Li, H.M., Theg, S.M., Bauerle, C.M., and Keegstra, K. (1990). Metal-ion-center assembly of ferredoxin and plastocyanin in isolated chloroplasts. Proc. Natl. Acad. Sci. USA **87,** 6748–6752.

Lin, S.J., Pufahl, R.A., Dancis, A., O'Halloran, T.V., and Culotta, V.C. (1997). A role for the *Saccharomyces cerevisiae* ATX1 gene in copper trafficking and iron transport. J. Biol. Chem. **272,** 9215–9220.

Marschner, H. (1995). Mineral Nutrition of Higher Plants. (London: Academic Press).

Merchant, S., and Bogorad, L. (1986). Rapid degradation of apoplastocyanin in Cu(II)-deficient cells of *Chlamydomonas reinhardtii*. J. Biol. Chem. **261,** 15850–15853.

Merchant, S., and Dreyfuss, B.W. (1998). Posttranslational assembly of photosynthetic metalloproteins. Annu. Rev. Plant Physiol. Plant Mol. Biol. **49,** 25–51.

Moseley, J., Allinger, T., Herzog, P., Wehinger, E., Merchant, S., and Hippler, M. (2002). Adaptation to Fe-deficiency requires re-modelling of the photosynthetic apparatus. EMBO J. **21,** 6709–6720.

Müller, P., Li, X.-P., and Niyogi, K.K. (2001). Non-photochemical quenching: A response to excess light energy. Plant Physiol. **125,** 1558–1566.

Murashige, T., and Skoog, F. (1962). A revised medium for rapid growth and bioassays with tobacco tissue culture. Physiol. Plant. **15,** 437–497.

Murphy, A., and Taiz, L. (1995). A new vertical mesh transfer technique for metal-tolerance studies in Arabidopsis. Plant Physiol. **108,** 29–38.

Nelson, N. (1999). Metal ion transporters and homeostasis. EMBO J. **18,** 4361–4371.

Niyogi, K.K., Grossman, A.R., and Björkman, O. (1998). Arabidopsis mutants define a central role for the xanthophyll cycle in the regulation of photosynthetic energy conversion. Plant Cell **10,** 1121–1134.

Petrovic, N., Comi, A., and Ettinger, M.J. (1996). Identification of an apo-superoxide dismutase (Cu,Zn) pool in human lymphoblasts. J. Biol. Chem. **271,** 28331–28334.

Phung, L.T., Ajlani, G., and Haselkorn, R. (1994). P-type ATPase from the cyanobacterium *Synechococcus* 7942 related to the human Menkes and Wilson disease gene products. Proc. Natl. Acad. Sci. USA **91,** 9651–9654.

Pilon, M., de Kruijff, B., and Weisbeek, P. (1992). New insights into the import mechanism of the ferredoxin precursor into chloroplasts. J. Biol. Chem. **267,** 2548–2556.

Pilon-Smits, E.A.H., Garifullina, G.F., Abdel-Ghany, S.E., Kato, S.-I., Mihara, H., Hale, K.L., Burkhead, J.L., Esaki, N., Kurihara, T., and Pilon, M. (2002). Characterization of a NifS-like chloroplast protein from *Arabidopsis thaliana*: Implications for its role in sulfur and selenium metabolism. Plant Physiol. **130,** 1309–1318.

Pufahl, R.A., Singer, C.P., Peariso, K.L., Lin, S.-J., Schmidt, P.J., Fahrni, C.J., Culotta, V.C., Penner-Hahn, J.E., and O'Halloran, T.V. (1997). Metal ion chaperone function of the soluble Cu(I) receptor Atx1. Science **278,** 853–856.

Rae, T.D., Schmidt, P.J., Pufahl, R.A., Culotta, V.C., and O'Halloran, T.V. (1999). Undetectable intercellular free copper: The requirement

of a copper chaperone for superoxide dismutase. Science **284,** 805–808.

Raven, J.A., Evans, M.C.W., and Korb, R.E. (1999). The role of trace metals in photosynthetic electron transport in O_2-evolving organisms. Photosynth. Res. **60,** 111–149.

Rensink, W.A., Pilon, M., and Weisbeek, P. (1998). Domains of a transit peptide required for in vivo import into Arabidopsis chloroplasts. Plant Physiol. **118,** 691–700.

Rodriguez, F.I., Esch, J.J., Hall, A.E., Binder, B.M., Schaller, G.E., and Bleecker, A.B. (1999). A copper cofactor for the ethylene receptor ETR1 from Arabidopsis. Science **283,** 996–998.

Sambrook, J., Fritsch, E.F., and Maniatis, T. (1989). Molecular Cloning: A Laboratory Manual. (Cold Spring Harbor, NY: Cold Spring Harbor Laboratory Press).

Sancenon, V., Puig, S., Mira, H., Thiele, D.J., and Penarrubia, L. (2003). Identification of a copper transporter family in *Arabidopsis thaliana*. Plant Mol. Biol. **51,** 577–587.

Schreiber, U., Klughammer, C., and Neubauer, C. (1988). Measuring P700 absorbance changes around 830 nm with an new type of pulse modulation system. Z. Naturforsch. **43c,** 686–698.

Schreiber, U., Schliwa, U., and Bilger, W. (1986). Continuous recording of photochemical and non-photochemical chlorophyll fluorescence quenching with a new type of modulation fluorometer. Photosynth. Res. **10,** 51–62.

Schubert, M., Petersson, U.A., Haas, B.J., Funk, C., Schroder, W.P., and Kieselbach, T. (2002). Proteome map of the chloroplast lumen of *Arabidopsis thaliana*. J. Biol. Chem. **277,** 8354–8365.

Shikanai, T., Munekage, Y., Shimizu, K., Endo, T., and Hashimoto, T. (1999). Identification and characterization of *Arabidopsis* mutants with reduced quenching of chlorophyll fluorescence. Plant Cell Physiol. **40,** 1134–1142.

Smeekens, S., Baurle, C., Hageman, J., Keegstra, K., and Weisbeek, P. (1986). The role of the transit peptide in the routing of precursors toward different chloroplast compartments. Cell **46,** 365–375.

Smeekens, S., de Groot, M., van Binsbergen, J., and Weisbeek, P. (1985). Sequence of the precursor of the thylakoid lumen protein plastocyanin. Nature **317,** 456–458.

Solioz, M., and Vulpe, C. (1996). CPx-type ATPases: A class of P-type ATPases that pump heavy metals. Trends Biochem. Sci. **21,** 237–241.

Spiller, S., and Terry, N. (1980). Limiting factors in photosynthesis. II. Iron stress diminishes photochemical capacity by reducing the number of photosynthetic units. Plant Physiol. **65,** 121–125.

Tabata, K., Kashiwagi, S., Mori, H., Ueguchi, C., and Mizuno, T. (1997). Cloning of a cDNA encoding a putative metal-transporting P-type ATPase from *Arabidopsis thaliana*. Biochem. Biophys. Acta **1326,** 1–6.

Terry, N. (1980). Limiting factors in photosynthesis. I. Use of iron stress to control photochemical capacity *in vivo*. Plant Physiol. **65,** 114–120.

Tottey, S., Rich, P.R., Rondet, S.A.M., and Robinson, N.J. (2001). Two Menkes-type ATPases supply copper for photosynthesis in *Synechocystis* PCC6803. J. Biol. Chem. **276,** 19999–20004.

Tottey, S., Rondet, S.A.M., Borrelly, G.P.M., Robinson, P.J., Rich, P.R., and Robinson, N.J. (2002). A copper metallochaperone for photosynthesis and respiration reveals metal-specific targets, interaction with an importer and alternative sites for copper acquisition. J. Biol. Chem. **277,** 5490–5497.

Tsang, E.W.T., Bowler, C., Hérouart, D., Van Camp, W., Villarroel, R., Genetello, C., Van Montague, M., and Inzé, D. (1991). Differential regulation of superoxide dismutases in plants exposed to environmental stress. Plant Cell **3,** 783–792.

Van Camp, W., Capiau, K., Van Montagu, M., Inzé, D., and Slooten, L. (1996). Enhancement of oxidative stress tolerance in transgenic tobacco plants overproducing Fe-superoxide dismutase in chloroplasts. Plant Physiol. **112,** 1703–1714.

Vorst, O., Oosterhoff-Teertstra, R., Vankan, P., Smeekens, S., and Weisbeek, P. (1988). Plastocyanin of *Arabidopsis thaliana*: Isolation and characterization of the gene and chloroplast import of the precursor protein. Gene **65,** 59–69.

Williams, L.E., Pittman, J.K., and Hall, J.L. (2000). Emerging mechanisms for heavy metal transport in plants. Biochim. Biophys. Acta **1465,** 104–126.

Woeste, K.E., and Kieber, J.J. (2000). A strong loss-of-function mutation in *RAN1* results in constitutive activation of the ethylene response pathway as well as a rosette-lethal phenotype. Plant Cell **12,** 443–455.

Yuan, D.S., Stearman, R., Dancis, A., Dunn, T., Beeler, T., and Klausner, R.D. (1995). The Menkes/Wilson disease gene homologue in yeast provides copper to a ceruloplasmin-like oxidase required for iron uptake. Proc. Natl. Acad. Sci. USA **92,** 2632–2636.

Zhou, J., and Goldsbrough, P.B. (1994). Functional homologs of fungal metallothionein genes from Arabidopsis. Plant Cell **6,** 875–884.